miR-145 suppresses thyroid cancer growth and metastasis and targets *AKT3*

Myriem Boufraqech[1], Lisa Zhang[1], Meenu Jain[1], Dhaval Patel[1], Ryan Ellis[1], Yin Xiong[1], Mei He[1], Naris Nilubol[1], Maria J Merino[2] and Electron Kebebew[1]

[1]Endocrine Oncology Branch [2]Laboratory of Pathology, National Cancer Institute, National Institutes of Health, Center for Cancer Research, Bethesda, Maryland 20892, USA

Correspondence should be addressed to E Kebebew
Email
kebebewe@mail.nih.gov

Abstract

The expression and function of miR-145 in thyroid cancer is unknown. We evaluated the expression and function of miR-145 in thyroid cancer and its potential clinical application as a biomarker. We found that the expression of miR-145 is significantly downregulated in thyroid cancer as compared with normal. Overexpression of miR-145 in thyroid cancer cell lines resulted in: decreased cell proliferation, migration, invasion, VEGF secretion, and E-cadherin expression. miR-145 overexpression also inhibited the PI3K/Akt pathway and directly targeted *AKT3*. *In vivo*, miR-145 overexpression decreased tumor growth and metastasis in a xenograft mouse model, and VEGF secretion. miR-145 inhibition in normal primary follicular thyroid cells decreased the expression of thyroid cell differentiation markers. Analysis of indeterminate fine-needle aspiration samples showed miR-145 had a 92% negative predictive value for distinguishing benign from malignant thyroid nodules. Circulating miR-145 levels were significantly higher in patients with thyroid cancer and showed a venous gradient. Serum exosome extractions revealed that miR-145 is secreted. Our findings suggest that miR-145 is a master regulator of thyroid cancer growth, mediates its effect through the PI3K/Akt pathway, is secreted by the thyroid cancer cells, and may serve as an adjunct biomarker for thyroid cancer diagnosis.

Key Words
- miR-145
- thyroid cancer
- AKT3
- metastasis
- biomarker

Endocrine-Related Cancer (2014) **21**, 517–531

Introduction

The most common types of thyroid cancer are of follicular cell origin and can be classified as well-differentiated thyroid cancer (WDTC), poorly differentiated thyroid cancer (PDTC), and anaplastic thyroid cancer (ATC). Although WDTC represents the majority of thyroid cancers, PDTC and ATC account for most thyroid cancer-related mortality. Their pathogenesis is poorly understood, and a significant subset of WDTC progresses to PDTC and ATC (Schlumberger 2007). Several activating somatic mutations, involving the MAPK pathway, are common in WDTC (papillary thyroid cancer (PTC) and follicular thyroid cancer (FTC)). *RET/PTC* (*TAS2R38*) rearrangements and *BRAF* or *RAS* mutations are present in approximately two-thirds of PTC cases (Theoharis *et al.* 2012) whereas in FTC, mutations in *RAS* and *PTEN*, or *PAX8/PPARγ* rearrangements, are more common (Theoharis *et al.* 2012). In addition to these mutations, mutations in *TP53* or *β-catenin* are frequent in ATC. Many of these mutations occur as mutually exclusive genetic events and can result in microRNA (miRNA) and epigenetic changes.

http://erc.endocrinology-journals.org
DOI: 10.1530/ERC-14-0077

Published by Bioscientifica Ltd.

miRNAs are short (~19–22 nucleotides), highly conserved noncoding RNA sequences that bind to the 3′-UTR of multiple transcripts. Several studies have demonstrated the role of miRNAs in physiologic and pathologic conditions, including evidence suggesting miRNA dysregulation in tumorigenesis (Solomides *et al.* 2012). Among the many miRNAs dysregulated in cancer, miR-145 has been proposed to be a tumor suppressor in several cancers. miR-145 is downregulated in breast, prostate, and colon cancers and is involved in cell differentiation and proliferation (Akao *et al.* 2006, Volinia *et al.* 2006, Sachdeva *et al.* 2009). Several investigators have reported that dysregulated miRNA expression in WDTC, PDTC, and ATC. Distinct miRNA expression profiles have been associated with mutational status and disease-aggressiveness (Pallante *et al.* 2006, 2014, de la Chapelle & Jazdzewski 2011, Kitano *et al.* 2012). However, the biological role of miR-145 in thyroid cancer has not been studied. The aim of this study was to characterize the expression of miR-145 in thyroid cancer, identify its function in thyroid cancer cells *in vitro* and *in vivo*, and to determine its utility in thyroid cancer diagnosis.

Materials and methods

Tissue samples

Thyroid tissue was obtained at the time of surgical resection, snap-frozen, and stored at −80 °C. Serial sections of tissue samples were stained with hematoxylin–eosin and reviewed by a pathologist to confirm the diagnosis and to ensure that the tumor tissue content was >80%. Thyroid fine-needle aspiration (FNA) biopsy samples were obtained on a clinical protocol. The cytologic diagnoses were classified according to The Bethesda System for Reporting Thyroid Cytopathology (Cibas & Ali 2009). To determine the accuracy of miR-145 expression levels in distinguishing between benign and malignant thyroid nodules, a training and validation set of samples with inconclusive FNA diagnosis was used. The validation was performed blinded to the histologic diagnosis and clinical data. The clinical protocol for tissue and thyroid FNA biopsy procurement was approved by the National Cancer Institute central institutional review board and written informed consent was obtained from all subjects.

Cell culture and reagents

The TPC-1 cell line (originated from PTC) was provided by Dr Nabuo Satoh (Japan), the FTC-133 cell line was provided by Dr Peter Goretzki (Germany), and the ATC cell line 8505C was purchased from European Collection of Cell Cultures (ECACC, Salisbury, UK). The cell lines were maintained in DMEM supplemented with 10% serum, penicillin, streptomycin, and fungizone (250 mg/ml). The cell lines were authenticated by short-tandem repeat profiling.

The culture of primary thyroid follicular cells was prepared by mincing fresh normal thyroid tissue into small fragments. The fragments were digested with collagenase (100 U/ml) (Invitrogen, Life Technologies) and protease dispase II (2.4 U/ml) (Roche Applied Science). The cells were maintained in Ham's F-12 culture medium supplemented with 5% (w/v) fetal calf serum (FCS) (GE Healthcare, Buckinghamshire, UK), 2 mM L-glutamine (Invitrogen), 1% NEAA (Invitrogen), 1 U/l bovine thyroid-stimulating hormone (TSH) (Sigma–Aldrich), 10 mg/l human insulin (Roche Applied Science), 10 mg/l somatostatin (Sigma–Aldrich), 6 mg/l human transferrin (Roche Applied Science), and 10^{-8} M hydrocortisone (Roche Applied Science).

For the evaluation of the PI3K/Akt pathway, cells were treated with 50 μM of LY294002 (Invitrogen) for 48 h, and protein and RNA were harvested. To evaluate exosomes secretion, cells were treated with inhibitors of protein transport and secretion: i) brefeldin A (BFA), a fungal metabolite demonstrated to inhibit anterograde transport from the endoplasmic reticulum to the Golgi apparatus (Affymetrix, eBiosciences, San Diego, CA, USA) for 14–16 h, or ii) GW4869 (Sigma–Aldrich), a ceramide inhibitor for 24 h. The cells and the culture medium were harvested for miRNA and exosome extraction.

Cell transfection

miR-145 mimic or inhibitor and negative control miRNA (*mir*Vana miRNA mimic/inhibitor, Life Technologies) were transiently transfected into thyroid cell lines in six-well plates using RNAiMax (Life Technologies) according to the manufacturer's protocol.

Cell proliferation

The cells were transfected in 96-well plate and the CyQUANT assay kit (Life Technologies) was used to evaluate cell proliferation according to the manufacturer's instructions.

RNA extraction and real-time RT-PCR

Total RNA was extracted from snap-frozen tissues and cell lines using TRIZol reagent (Life Technologies), according to the manufacturer's protocol. RNA yield was determined

http://erc.endocrinology-journals.org
DOI: 10.1530/ERC-14-0077

Published by Bioscientifica Ltd.

using the NanoDrop 2000 (Thermo Scientific, Wilmington, DE, USA).

For miRNA detection, 5 ng of total RNA were reverse transcribed using the microRNA Reverse Transcription Kit (Life Technologies), followed by RT-PCR. U6 snRNA was used as an endogenous control. For gene expression, 500–1000 ng of total RNA was reverse-transcribed using a High Capacity Reverse Transcription cDNA Kit (Life Technologies), and cDNA was diluted and amplified according to the manufacturer's instructions (Life Technologies). *GAPDH* was used as endogenous control. miRNA and gene expression levels were calculated using SDS 2.3 software (Life Technologies).

The relative expression of each gene was normalized to that of the housekeeping gene and calculated using the $2^{-\Delta Ct}$ method for *in vitro* studies and the $-\Delta Ct$ method for human samples.

Wound-healing assay

At ~90% confluence, the monolayer of cells was scratched with a sterile plastic tip. The cells were then cultured for up to 20 h and imaged by an inverted microscope to measure wound assay width (Carl Zeiss, Inc., Oberkochen, Germany).

Cellular invasion and migration assay

Cellular invasion and migration were determined using the Transwell chamber assay (BD Biosciences, San Jose, CA, USA), according to the manufacturer's protocol, with and without matrigel respectively. After 22 h of incubation at 37 °C, the cells invading through the bottom surface of the inserts were fixed, stained with Diff-Quik (Dade Behring, Newark, NJ, USA), and photographed and counted using Image J software (National Institutes of Health, Bethesda, MD, USA).

Immunohistochemistry

Deparaffinized and rehydrated sections were incubated with the primary antibodies for VEGF (AbCam, Cambridge, England, Supplementary Table 1, see section on supplementary data given at the end of this article) and proliferating cell nuclear antigen (PCNA) (Santa Cruz Biotechnology, Supplementary Table 1) at 1:100 dilution for 2 h at room temperature (RT), followed by incubation with a secondary antibody for 1 h at RT. The whole slides were scanned at 20× magnification using a ScanScope XT digital slide scanner and viewed using ImageScope software (Aperio Technologies, Inc., Vista, CA, USA).

Cell cycle assay

The transfected cells were harvested, fixed with cold 70% ethanol for 30 min at 4 °C, and incubated in the dark with RNase (100 μg/ml) and propidium iodide (50 μg/ml) for 30 min at 37 °C. A total of 20 000 nuclei were examined by flow cytometry using a Calibur flow cytometer (Becton-Dickinson, Franklin Lakes, NJ, USA), and data were analyzed using ModFit software (Verity Software House, Topsham, ME, USA).

Apoptosis assay

Apoptosis was analyzed using Apo-BrdU staining. DNA strand breaks were stained with FITC-conjugated anti-BrdU MAB according to the manufacturer's protocol (BD Pharmingen, San Diego, CA, USA). Caspase-Glo 3/7 assay (Promega) was used to measure caspase activity after 72 h of transfection according to the manufacturer's protocol.

Western blot analysis

The total protein lysate was analyzed by SDS–PAGE, transferred to a nitrocellulose membrane, and immunostained with the following antibodies overnight at 4 °C: anti-vimentin (1:1000, AbCam Supplementary Table 1); anti-CD44 (1:1000, Cell Signaling Technology, Beverly, MA, USA, Supplementary Table 1); anti-p-Akt^{Ser473} (1:1000, Cell Signaling Technology, Supplementary Table 1); anti-CDC25C (1:1000, Cell Signaling Technology); anti-cyclin D1 (1:1000, Cell Signaling Technology, Supplementary Table 1); anti-N-cadherin (1:1000, EMD Millipore, Billerica, MA, USA Supplementary Table 1); anti-GAPDH (1:5000, Santa Cruz Biotechnology, Supplementary Table 1); and anti-p21 (1:250, Santa Cruz Biotechnology, Supplementary Table 1). Anti-human GAPDH (1:5000, Santa Cruz Biotechnology, Supplementary Table 1) was used as a loading control. The membranes were incubated with the appropriate HRP-conjugated IgG (anti-rabbit 1:3000, Cell Signaling Technology, or anti-mouse 1:10 000, Santa Cruz Biotechnology, Supplementary Table 1), and proteins were detected by ECL (Thermo Scientific, Rockford, IL, USA, Supplementary Table 1).

ELISA test

Culture media were collected and the VEGF ELISA was carried out using Quantikine Human VEGF Immunoassay, according to the manufacturer's instruction (R&D Systems, Minneapolis, MN, USA). The amount of VEGF

http://erc.endocrinology-journals.org
DOI: 10.1530/ERC-14-0077

Published by Bioscientifica Ltd.

protein was compared with total protein as determined with the BCA reagent (Thermo Scientific).

Luciferase assay

The cells were seeded in triplicate in 96-well plate and cultured for 24 h. The pLightSwitch 3′-UTR Reporter gene plasmid, pLightSwitch-Akt3-3′-UTR, was co-transfected with miR-C mimic or miR-145 mimic (*miRVana,* Applied Biosystems) into cells using Lipofectamine 2000 Reagent (Life Technologies). Luciferase activity was measured 24 h after transfection using the LightSwitch Luciferase Assay Kits (Switchgear Genomics, Carlsbad, CA, USA) according to the manufacturer's instructions.

Xenografts studies in mice

Animal studies were approved by the National Cancer Institute's Institutional Animal Care and Use Committee. The mice were maintained according to the guidelines of the National Cancer Institute's Animal Research Advisory Committee. Briefly, 8505C cells were stably transfected with linearized pGL4.51[luc2/CMV/Neo] vector luciferase reporter (8505C-Luc cells) and transiently transfected with miR-C or miR-145. Into the flanks of nude mice, 1.6×10^6 cells of 8505C-Lucin in 100 μl DMEM were injected subcutaneously. Tumors were measured every week and recorded in mm^3. For evaluating lung metastasis, 90 000 8505C-Luc cells were injected into the tail vein of Cg-*Prkdc*^{scid}*Il2rg*^{tm1Wjl}/SzJ mice. The mice were intraperitoneally injected with 30 mg/ml of luciferin and imaged. The images were analyzed using IVIS Living Image software (Caliper Life Sciences, Inc., Hopkinton, MA, USA).

RNA extraction from serum and culture medium

The culture media and serum samples were centrifuged at 3166 ***g*** for 30 min, miRNAs were extracted from 200 μl of the supernatant using the miRNeasy Extraction Kit (Qiagen). The exosomes were extracted from cell culture media and serum using the Total Exosomes Isolation Kit (Life Technologies) according to the manufacturer's protocol. About 2 μl of isolated miRNA were reverse transcribed using the microRNA Reverse Transcription Kit followed by RT-PCR. miR-16 was used as an endogenous control.

Statistical analyses

Statistical analyses were performed using the GraphPad Prism 5 software (GraphPad Software, La Jolla, CA, USA). Parametric and nonparametric data were analyzed using a two-tailed *t*-test and the Mann–Whitney *U* test respectively. $P<0.05$ was considered statistically significant. Data are presented as mean ± S.D. or mean ± S.E.M.

Results

miR-145 is downregulated in thyroid cancer

We found miR-145 expression was downregulated in WDTC and PDTC/ATC ($P<0.0001$ and $P=0.0013$ respectively) compared with normal thyroid tissue (Fig. 1A). *In vitro* studies showed that levels of miR-145 were low in TPC1 and 8505C cells, whereas FTC-133 demonstrated relatively high levels of miR-145 compared with the other cell lines (Table 1).

miR-145 decreases cell proliferation and induces cell cycle arrest

Because miR-145 was downregulated in thyroid cancer cell lines, we induced the overexpression of miR-145 mimic or miR-C. Successful transfection was validated by RT-PCR (Supplementary Figure 1, see section on supplementary data given at the end of this article). Overexpression of miR-145 inhibited cellular proliferation compared with negative control (miR-C) (Fig. 1B). Cell cycle analysis by flow cytometry showed that miR-145 induced G2/M cell cycle arrest (Fig. 1C, Supplementary Figure 2). Because phosphorylation of p21 by p-Akt modulates cell cycle and apoptosis by decreasing the binding of cyclin-dependent kinases, CDK2 and CDK4, to p21, we hypothesized that miR-145 may regulate cell cycle by altering p21 expression. Indeed, we found p21 was higher with overexpression of miR-145 (Fig. 1D). miR-145 overexpression also decreased cyclin D1 expression (Fig. 1D). CDC25C plays a critical role in the G2/M checkpoint by dephosphorylating CDC2. Expression of CDC25 was decreased with miR-145 overexpression as compared with miR-C overexpression (Fig. 1D). Thus, miR-145 regulates cell cycle progression by modulating the expression of multiple key proteins regulating cell cycle and cell proliferation.

miR-145 induces caspase-dependent apoptosis

Although miR-145 overexpression resulted in G2/M arrest, this effect did not fully account for the effect on cellular proliferation we observed in the thyroid cancer cell lines. Thus, we postulated that miR-145 may also have an effect on apoptosis. We assessed the activation of apoptosis by Apo-BrdU labeling and found increased DNA

http://erc.endocrinology-journals.org
DOI: 10.1530/ERC-14-0077

Published by Bioscientifica Ltd.

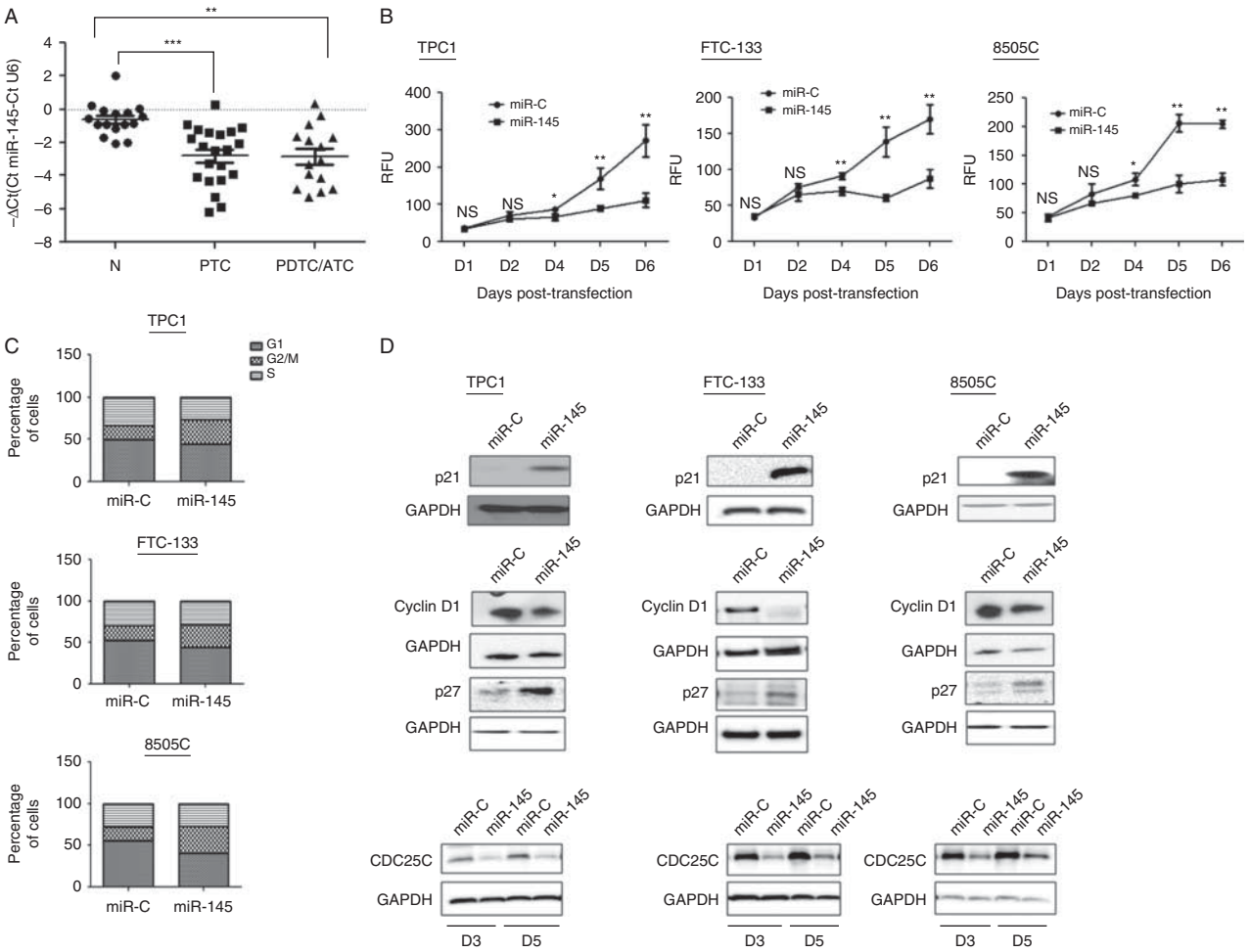

Figure 1

Expression of miR-145 in thyroid tissue samples and thyroid cancer cell lines and the effect of miR-145 overexpression in the thyroid cancer cell lines. (A) Normalized relative expression of miR-145 by tissue type is shown in the scatter plot. 16 normal, 21 PTC, and 15 ATC/PDTC tissue samples were analyzed. miR-145 expression was significantly decreased in PTC ($P=0.0001$) and PDTC/ATC ($P=0.0013$). N, normal; PTC, papillary thyroid cancer; PDTC, poorly differentiated thyroid cancer; ATC, anaplastic thyroid cancer. ***$P<0.001$. (B) Cell proliferation was determined in the TPC1, FTC-133, and 8505C cell lines using Cyquant assay every 24 h after transfection with 35 nM miR-145 or miR-C. miR-145 transfection significantly inhibited cell proliferation, as compared with miR-C transfection. *$P<0.05$; **$P<0.001$. (C) Cell cycle analysis with miR-145 and miR-C transfection. G2/M arrest was increased by miR-145 overexpression. The results represent three independent experiments. (D) miR-145 modulates cell cycle regulatory proteins. Western blot analysis showed changes in cyclin D1, p21, p27, and CDC25C, consistent with G2/M arrest.

fragmentation with overexpression of miR-145 (Fig. 2A). Furthermore, the activity of CASP3/CASP7, which plays central roles in apoptosis, was also significantly higher with overexpression of miR-145, suggesting that the effect of miR-145 on apoptosis is caspase dependent (Fig. 2B).

miR-145 regulates cellular invasion and migration, and EMT marker expression

Previous studies have shown that WDTC progresses to ATC and PDTC as a result of epithelial–mesenchymal transition (EMT) (Zhong *et al*. 2005, Patel & Shaha 2006), which is accompanied by altered cellular morphology and increased cell spreading (De Craene & Berx 2013). Given the findings of low levels of miR-145 in PDTC and ATC, we postulated that miR-145 may mediate EMT and carried out *in vitro* studies investigating cellular invasion and migration. miR-145 overexpression resulted in a significant inhibition of invasion and migration in all three thyroid cancer cell lines (Fig. 3A). In addition, inhibition of miR-145 expression in the FTC-133 cell line, which expresses a higher level of miR-145, increased

http://erc.endocrinology-journals.org
DOI: 10.1530/ERC-14-0077

Published by Bioscientifica Ltd.

Table 1 Basal expression of miR-145 in thyroid cancer cell lines TPC1, FTC-133, 8505C, and primary thyroid culture

Cell line	Ct (miR-145)
TPC1	35.9
FTC-133	22.9
8505C	35
Primary culture	20.1

invasion (Fig. 3B). miR-145 overexpression also significantly decreased the wound closure rate (Fig. 3C) and resulted in the downregulation of EMT marker N-cadherin in 8505C and TPC1 cell lines. However, miR-145 overexpression did not affect N-cadherin expression levels in the *PTEN*-deficient FTC-133 cell line (Fig. 3D), and had no effect on E-cadherin and vimentin levels (data not shown).

Restoration of miR-145 expression downregulates stem cell markers and induces expression of follicular thyroid cell differentiation markers

Dedifferentiation of thyroid cancer results in the loss of thyroid-specific gene expression and reduces the efficacy of adjuvant therapies, such as radioiodine ablation, which requires the expression of the sodium iodide symporter (*NIS*). The transcription factor, *PAX8*, located in the regulatory region of the *NIS* promoter/enhancer, is frequently dysregulated in advanced cancers and is a marker of follicular thyroid differentiation status (Lacroix *et al.* 2006). Given the loss of miR-145 expression in PDTC and ATC, and the effect of miR-145 on EMT marker expression, cellular invasion, and migration, we reasoned that miR-145 may modulate follicular thyroid cell

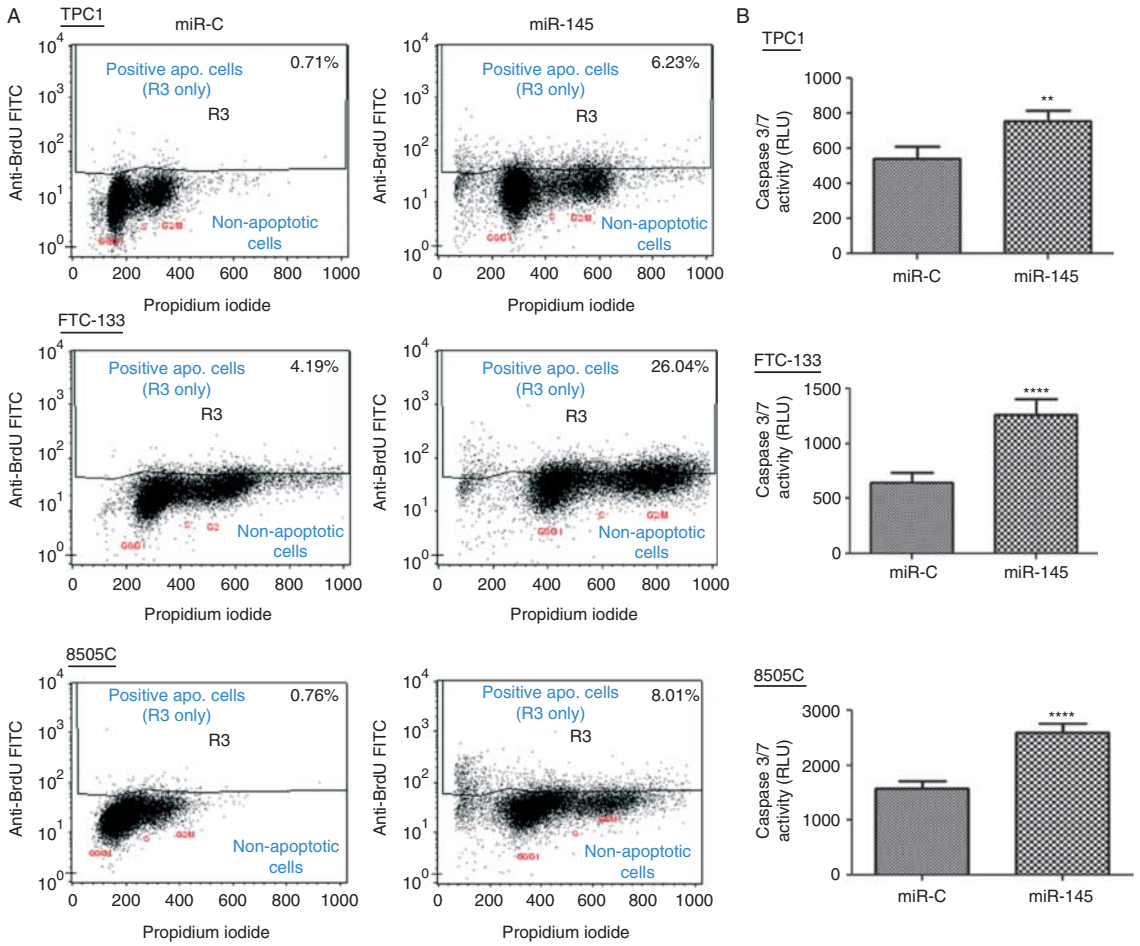

Figure 2

Effects of miR-145 on apoptosis. (A) miR-145 increases apoptosis. 72 h after transfection with miR-145 or miR-C, DNA fragmentation in cells was measured using Apo-BrdU labeling as described in Materials and methods. These data represent three independent experiments. (B) miR-145 increases caspase 3/7 activity. Three days after transfection, caspase 3/7 activity in miRNA-transfected cells was measured. The error bars represent ±s.d. from three different experiments. $^{**}P<0.01$; $^{****}P<0.0001$.

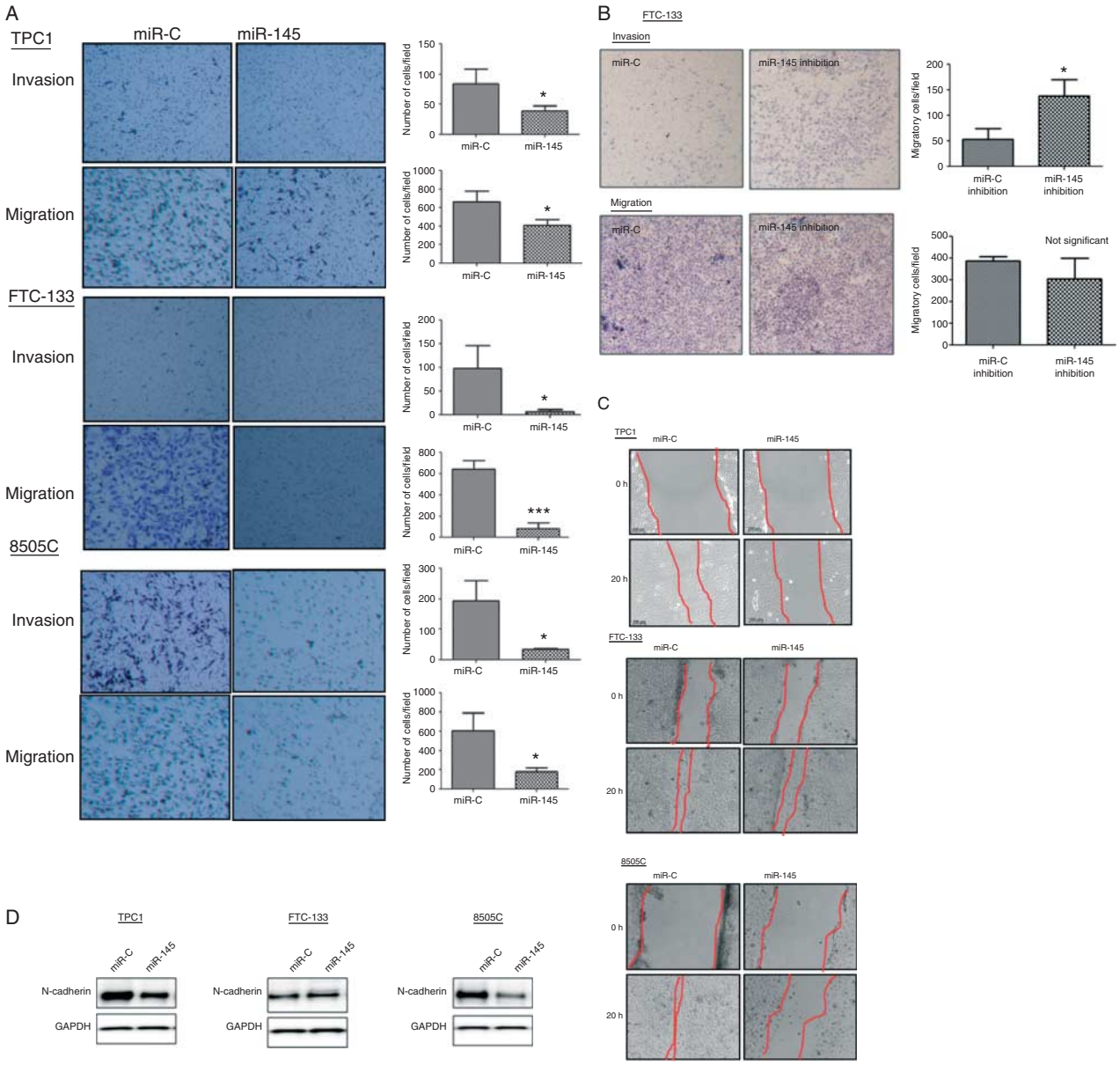

Figure 3

Overexpression of miR-145 inhibits EMT markers' expression, and cellular migration and invasion *in vitro*. (A) Transwell migration and matrigel invasion assay. The images show the cells that penetrated the matrigel (invasion) and those that penetrated the inserts' membrane (migration). Ectopic expression of miR-145 inhibited migration and invasion in thyroid cancer cell lines 72 h after transfection (left panel). The migratory and invasive cells from three independent experiments were counted, and are presented with the S.D. (right panel) (*$P<0.05$; ***$P<0.001$). (B) Inhibition of miR-145 in FTC-133 increased cell invasion but had no significant effect on cell migration. The migratory and invasive cells from three independent experiments were counted and are presented ±S.D. (right panel) (*$P<0.05$; ***$P<0.001$). (C) Representative images of scratch wound–healing migration assay in thyroid cancer cell lines transfected with miR-145 or miR-C. (D) N-cadherin (antibody ref) expression decreases with miR-145 transfection, as compared with miR-C.

differentiation. Indeed, inhibition of miR-145 in primary cultures of normal thyroid tissue samples was accompanied by a decrease in *NIS* and *PAX8* and *TPO* expression (Fig. 4A). Thus, we examined the association between miR-145 expression, and *NIS*, *PAX8,* and thyroglobulin (*TG*) expression. In thyroid cancer samples with low miR-145 expression, we found low *NIS* and *TG* expression (Fig. 4B). However, *PAX8* expression levels did not have a significant correlation with miR-145 expression (data not shown).

http://erc.endocrinology-journals.org
DOI: 10.1530/ERC-14-0077

Published by Bioscientifica Ltd.

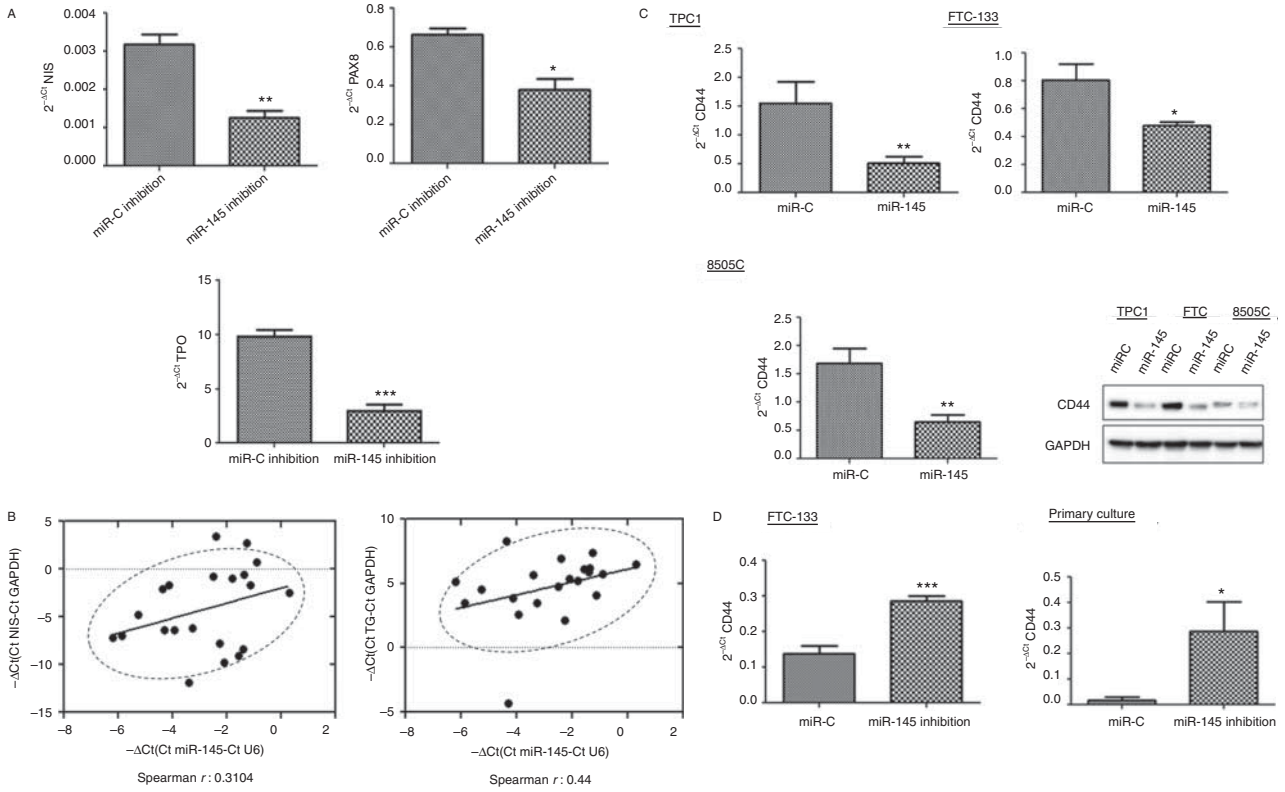

Figure 4
miR-145 regulates the expression of cell differentiation markers. (A) RT-PCR analysis of NIS PAX8 and TPO expression in normal primary culture transfected with miR-145 inhibitor, $n=3$. (B) Correlation of miR-145 expression with NIS and TG expression in PTC samples. (C) Quantitative real-time PCR analysis of CD44 mRNA expression in thyroid cancer cells with miR-145 transfection vs miR-C. Relative mRNA expression was normalized to GAPDH. Western blot analysis and quantification of CD44 expression in miR-145-transfected and miR-C-transfected thyroid cell lines. GAPDH was used as a loading control. (D) Quantitative real-time PCR analysis of CD44 mRNA expression with miR-145 inhibitor transfection vs miR-C inhibitor in FTC-133 cells and in normal primary thyrocyte culture. Each gene was normalized to the housekeeping gene and the relative expression was calculated using $2^{-\Delta Ct}$ method for *in vitro* studies and $-\Delta Ct$ method for tissue samples. $^{*}P<0.05$, $^{**}P<0.01$, $^{***}P<0.001$.

Since cellular dedifferentiation is often accompanied by overexpression of cancer stem cell markers, such as *CD44*, we investigated whether miR-145 affected *CD44* expression levels. Overexpression of miR-145 decreased *CD44* expression in thyroid cancer cell lines (Fig. 4C). In contrast, inhibition of miR-145 in FTC-133 in normal primary thyroid culture increased the expression of *CD44* (Fig. 4D). Taken together, these data suggest that loss of miR-145 expression is involved in follicular thyroid cell differentiation.

miR-145 expression inhibits Akt signaling in thyroid cancer cells

As overexpression and inhibition of miR-145 in thyroid cancer cell lines and normal primary thyroid culture had multiple effects on the hallmarks of cancer, we postulated that miR-145 may mediate these effects through a central pathway important in thyroid cancer initiation and progression. Because the majority of thyroid cancers of follicular cell origin have activating mutations involving the MAPK pathway with *BRAF*, *RET/PTC*, or *RAS* mutation (Theoharis *et al*. 2012) and the PI3K/Akt pathway, we tested the hypothesis that the effect of miR-145 could be mediated through these two pathways. We observed miR-145 overexpression decreased p-Akt expression (Fig. 5A) but had no effect on the ERK/MEK pathway (Supplementary Figure 3A, see section on supplementary data given at the end of this article) in TPC1 and 8505C. Akt3 is a predicted target of miR-145 through a potential binding site within the 3′-UTR region (Supplementary Figure 3C). AKT3 protein expression was significantly reduced by overexpression of miR-145 in the thyroid cancer cell lines (Fig. 5B) whereas AKT1 and AKT2 expression was not

http://erc.endocrinology-journals.org
DOI: 10.1530/ERC-14-0077

Published by Bioscientifica Ltd.

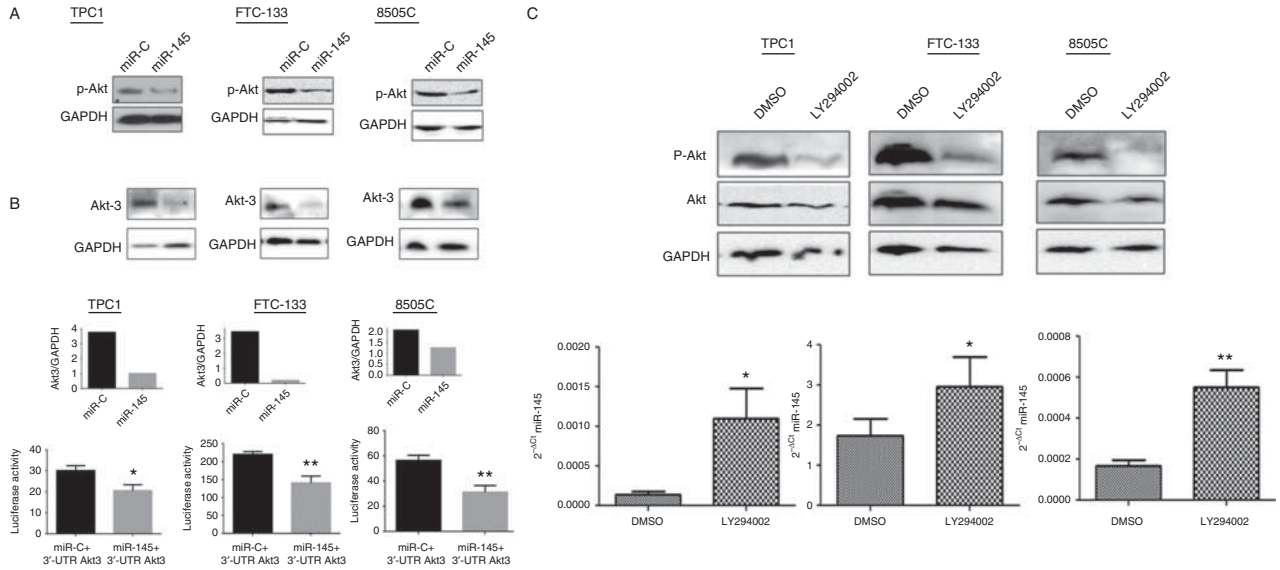

Figure 5

Overexpression of miR-145 attenuates the PI3K/Akt pathway. (A) Transient transfection of miR-145 decreased the phosphorylation of Akt on serine^{473} 3 days after transfection. (B) miR-145 decreased Akt3 expression. Luciferase vector was designed to include the region of the candidate target sequence for miR-145. Luciferase activity of 3′-UTR-Akt3 Luciferase vector after co-transfection with miR-C or miR-145 in three thyroid cancer cells. (C) miR-145 levels increase with PI3K/Akt inhibition using LY294002. Thyroid cancer cell lines were treated with 50 μM LY294002 for 48 h (*$P<0.05$, **$P<0.001$).

affected (Supplementary Figure 3B). To determine whether miR-145 binds to the Akt3 transcript, we performed luciferase reporter assay. Co-transfection of miR-145 and 3′-UTR-Akt3 significantly inhibited the luciferase activity (Fig. 5B). We also tested whether p-Akt was involved in silencing miR-145. Indeed, inhibition of PI3K-dependent Akt phosphorylation by LY294002 increased the expression of miR-145 in the thyroid cancer cell lines (Fig. 5C). Taken together, these findings suggest that miR-145 blocks the PI3K/Akt pathway, and this effect can be accentuated with PI3K/Akt pathway inhibitors, resulting in increased miR-145 levels. Although, we found decreased cellular invasion and migration with miR-145 overexpression in the FTC-133 cell line, there was no effect on cellular migration by the wound assay and in EMT marker expression (Fig. 3C and D), suggesting that EMT in the PTEN-deficient FTC-133 cell line is not only dependent on miR-145 levels. Indeed, overexpression of miR-145 increased p-MEK expression in FTC-133, suggesting an alternative pathway that may regulate EMT (Supplementary Figure 3A).

Overexpression of miRNA-145 inhibits tumor growth and metastasis *in vivo*

To determine whether overexpression of miR-145 inhibits tumor growth *in vivo*, 8505C cells expressing a luciferase reporter (Luc) were transfected with miR-145 mimic or miR-C, and injected subcutaneously into the flanks of nude mice. Xenografts overexpressing miR-145 resulted in slower tumor growth as compared with miR-C (Fig. 6A). Three weeks after injection, cells transfected with miR-145 showed luminescence intensity 75% lower than the control group (Fig. 6B). Four weeks after injection, xenograft tumors with miR-145 showed less immunohistochemical staining for PCNA than those with miR-C (Fig. 6C).

Because of the effect of miR-145 on cellular migration and invasion *in vitro*, we also evaluated if miR-145 alters tumor metastasis *in vivo*. 8505C cells expressing the luciferase reporter were transfected with miR-145 mimic or miR-C and injected into the tail vein of Cg-*Prkdc*^{scid}*Il2rg*^{tm1Wjl}/SzJ mice. The mice injected with 8505C-Luc miR-C had more prominent lung metastasis than those injected with 8505-Luc miR-145 mimic (Fig. 6D). Furthermore, the miR-C cells generated multiple distant metastases to the liver, kidneys, bone, and spleen, whereas miR-145-expressing cells showed fewer sites of distant metastases (only to the bone and spleen) (Supplementary Figure 4, see section on supplementary data given at the end of this article). Histologic analysis using PCNA as a proliferation marker and bioluminescence imaging confirmed that miR-145 reduced tumor metastases

http://erc.endocrinology-journals.org
DOI: 10.1530/ERC-14-0077

Published by Bioscientifica Ltd.

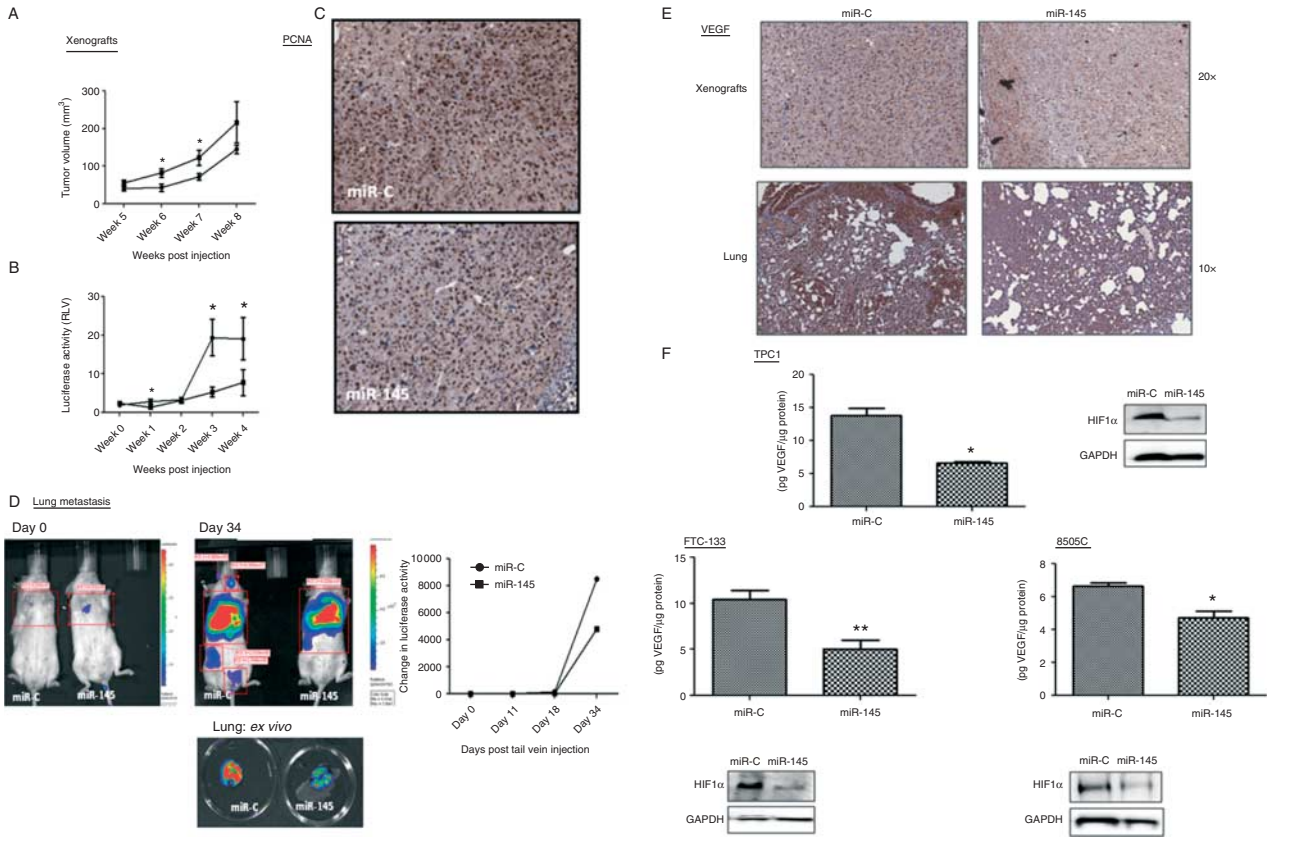

Figure 6

Effect of miR-145 on tumor growth and metastasis *in vivo*. Nude mice were injected subcutaneously with 8505C-luciferase cells expressing either miR-C or miR-145. (A and B) Tumor volume (mean ± S.E.M.) and luciferase activity (mean ± S.D.) were measured over time (*$P<0.05$; **$P<0.001$) (data from six mice with two injection sites per mouse). (C) Immunohistochemistry staining for PCNA expression in flank-xenografted tumor. Magnification ×20. Metastatic lesions in mice that had tail vein injection of 8505C-Luc cells. (D) Representative bioluminescence images of lung metastasis in mice with tail vein injection of cells overexpressing miR-145 or miR-C. Luciferase activity of metastasis in mice is presented in relative luminescence value (RLV). *$P<0.05$; **$P<0.001$. miR-145 decreases VEGF secretion. (E) Immunostaining for VEGF in xenografts and lung metastasis of mice injected with 8505C-Luc with miR-145 or miR-C transfection. (F) VEGF secretion and *HIF1α* expression with miR-145 transfection. Culture medium was collected at 72 h after transfection of miR-145 or miR-C in three thyroid cancer cell lines.

(Fig. 6D, Supplementary Figure 4A). Thus, these results suggest that miR-145 regulates metastasis.

miR-145 inhibits VEGF secretion *in vitro* and *in vivo*

Since the *in vivo* data indicate that miR-145 has a role in thyroid tumor growth and metastasis, and that it inhibits the PI3K–Akt pathway *in vitro*, a regulator of tumor angiogenesis, we tested whether miR-145 may also regulate VEGF secretion, a major mediator of angiogenesis. A comparison of the VEGF staining in xenograft metastatic tumors showed less staining in tumors with miR-145 overexpression (Fig. 6E). We next used ELISA to compare the VEGF secretion in thyroid cancer lines and found lower VEGF secretion in cells overexpressing miR-145 (Fig. 6F), which was also associated with reduced HIF1α expression (Fig. 6F).

miR-145 is a diagnostic marker in clinical thyroid FNA biopsy samples

Because of the loss of miR-145 expression in thyroid cancer, we explored the diagnostic utility of miR-145 expression in thyroid FNA biopsy. A predictive cutoff for miR-145 expression was developed using a training set of 22 FNA samples (Fig. 7A, upper panel). Quantitative RT-PCR was carried out in a validation set of 75 independent FNA samples classified as inconclusive on cytology. We observed a wider range of miR-145 expression levels in benign samples. Despite a considerable

http://erc.endocrinology-journals.org
DOI: 10.1530/ERC-14-0077

Published by Bioscientifica Ltd.

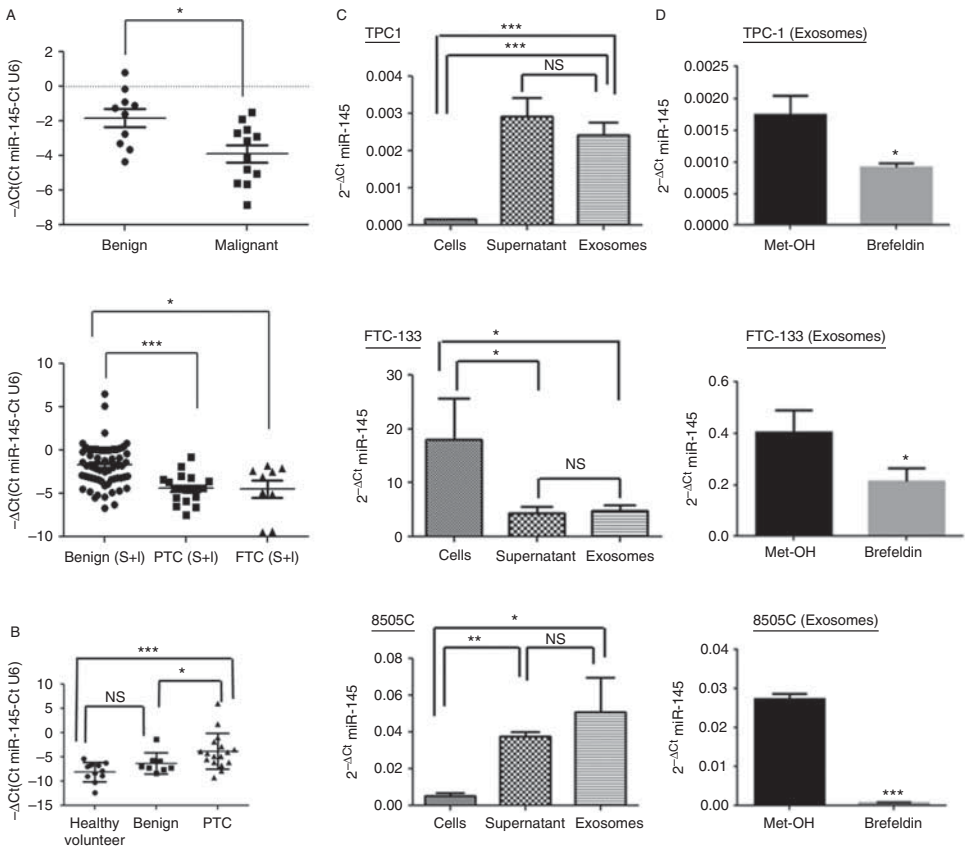

Figure 7

Expression levels of miR-145 in thyroid FNA biopsy samples. Normalized −ΔCt values for the training group (A upper panel) and validation group (A lower panel). *P* values were calculated using the Mann–Whitney *U* test. All the miR-145 Ct values were normalized to U6. miR-145 levels in serum samples and cell culture medium. (B) Serum level of miR-145 by RT-PCR in patients with PTC (17 samples), benign thyroid nodules (eight samples) as determined by histologic examination and 11 healthy volunteers blood donors. *P* values were calculated using the Mann–Whitney *U* test. (C) Level of miR-145 in cells, supernatant, and exosomes extracted from culture medium of three thyroid cancer cell lines using RT-PCR. The $2^{-\Delta Ct}$ values are presented as the mean ± s.d. ($n=3$). (D) miR-145 expression by RT-PCR in exosomes secreted by thyroid cancer cells treated with brefeldin A (12 h treatment for TPC1 and FTC133 and 16 h for 8505C). $^{*}P<0.05$, $^{**}P<0.01$, $^{***}P<0.001$.

overlap between malignant and benign samples, miR-145 was found to be significantly downregulated in malignant biopsy samples, as compared with benign ones (***$P<0.0001$ for PTC and *$P=0.014$ for FTC) (Fig. 7A, lower panel), with an overall sensitivity of 96%, specificity of 27%, positive predictive value (PPV) of 44%, negative predictive value (NPV) of 92%, and area under the ROC curve of 0.73. This finding suggests that miR-145 could be a helpful adjunct biomarker to FNA cytology for predicting benign lesions.

miR-145 serum levels are elevated in patients with thyroid cancer

Several investigators have reported elevated miRNA levels in serum samples in patients with cancer. This suggests that circulating miRNAs could be used as noninvasive diagnostic or prognostic markers (Mitchell *et al*. 2008, Ng *et al*. 2009). We found miR-145 levels were higher in serum samples from patients with PTC compared with individuals without cancer (Fig. 7B). We also carried out *in vitro* studies in the thyroid cancer cell line cultures to determine whether miR-145 is secreted by thyroid cancer cells. miRNAs extracted from the supernatant of thyroid cancer cell lines had much higher levels of miR-145 than intracellular levels in two of the three cell lines, suggesting miRNA secretion (Fig. 7C). The cell culture supernatant and exosome fraction had similar levels of miR-145. These data suggested that the elevated levels of miR-145 in serum samples from patients with PTC we observed may be in the exosome fraction (Fig. 7C), which was validated by the presence of CD63, a marker of exosomes.

Table 2 miR-145 levels in exosomes extracted from serum samples from the thyroid vein and peripheral blood in patients with papillary thyroid cancer

PTC	miR-145 Ct
Patient 1	
Local	25.6
Peripheral	33.5
Patient 2	
Local	28.4
Peripheral	30.6
Patient 3	
Local	29.6
Peripheral	34
Patient 4	
Local	21.5
Peripheral	22.6

All exosomes from the cell lines showed uniform CD63 expression (Supplementary Figure 5A, see section on supplementary data given at the end of this article). To confirm that miR-145 secretion was mediated by exosomes, we blocked exosomes production in thyroid cancer cell lines using BFA which inhibits the guanine nucleotide-exchange protein BIG2 and regulates the secretion of exosomes-like vesicles (Islam *et al.* 2007). BFA treatment reduced the secretion of CD63-containing exosomes (Supplementary Figure 5B) and miR-145 level in the exosomes (Fig. 7D). To further confirm that miR-145 was secreted via exosomes from thyroid cancer cells, we treated the cell lines with a ceramide inhibitor because it has been shown that exosome release is mediated by sphingolipid ceramide (Trajkovic *et al.* 2008). Treatment of thyroid cancer cells with 1 μM of GW4869, ceramide inhibitor, decreased miR-145 expression in exosomes (Supplementary Figure 5C). As expected, GW4869 treatment also decreased CD63 levels (Supplementary Figure 5D). To further show that the elevated miR-145 level in serum from patients with thyroid cancer results from secretion of miR-145 from the thyroid cancer cells, we measured miR-145 level in blood samples from veins adjacent to thyroid cancer and from peripheral serum samples in patients with PTC. Indeed, miR-145 levels in exosomes were higher in the thyroid vein draining the tumor than that in peripheral circulation. Taken together, these finding suggests that miR-145 is secreted from thyroid cancer cells (Table 2).

Discussion

Our data demonstrates that the expression level of miR-145 was significantly lower in PTC, PDTC, and ATC than that in normal thyroid tissue. The expression of miR-145 was shown to reduce the expression of differentiation markers, decrease cell proliferation, and induce cell cycle arrest and apoptosis consistent with data from other cancers (Xu *et al.* 2012, Zhang *et al.* 2013). miR-145 also regulated the expression of *VEGF in vivo* and *in vitro*. For the first time, we report that miR-145 directly targets AKT3 and reduces Akt phosphorylation and signaling through the PI3K/Akt, which is known to regulate thyroid cancer initiation and progression. This is the first study to also show that miR-145 may be a diagnostic biomarker in patients with thyroid cancer, and that it is secreted by thyroid cancer cells. Given the multiple effects of miR-145 on thyroid cancer cell phenotype *in vitro* and *in vivo*, we propose that miR-145 is a master regulator of thyroid cancer growth and metastasis, and likely mediates these effects through the PI3K/Akt pathway by targeting AKT3.

Several studies have established a link between high levels of EMT markers and the loss of cell polarity, reduced expression of cell–cell adhesion molecules, and increased capacity for metastasis (Yang *et al.* 2005, Spaderna *et al.* 2006). While the multistep process leading to EMT and tumor invasion is not completely defined, aberrant expression of cadherins and vimentin is considered one of the main events leading to EMT. Due to their ability to regulate and coordinate several genes/pathways, miRNAs have been shown to regulate the expression of EMT markers (Ceppi & Peter 2014). Our current study results show that miR-145 reduces N-cadherin expression and morphologic changes in cell shape due to the restoration of miR-145. However, we did not observe a difference in vimentin and E-cadherin expression with miR-145 overexpression. Thus, the effects of miR-145 on EMT in thyroid cancer cells are conclusive. Tumor neo-angiogenesis has been associated with metastases, invasion, and lower survival rates in many cancers, including thyroid cancer (Soh *et al.* 1997). High levels of serum VEGF and increased tissue expression of VEGF have been reported in patients with thyroid cancer (Viglietto *et al.* 1995, Soh *et al.* 1997, Tuttle *et al.* 2002), and VEGF is a target of miR-145 (Fan *et al.* 2012). Our data demonstrate that miR-145 regulates VEGF secretion *in vitro* and *in vivo* in thyroid cancer cells, and that miR-145 overexpression reduces distant metastasis. In addition to the effect of VEGF in angiogenesis, another important regulator of this process is hypoxia-inducible factor 1 (HIF1). Stabilized HIF1 protein is transported into the nucleus, where it binds to hypoxia response elements (HREs) on DNA and activates *VEGF* gene transcription. High expression of *HIF1α* has been reported in thyroid cancer and thyroid cancer cell lines

http://erc.endocrinology-journals.org
DOI: 10.1530/ERC-14-0077

Published by Bioscientifica Ltd.

(Burrows *et al*. 2010). Our findings indicate that miR-145 reduces HIF1α expression, thus suggesting another indirect pathway of VEGF regulation mediated by the effect of miR-145 on *HIF1α*. Furthermore, HIF1α, highly expressed in thyroid cancers, is regulated not only by hypoxia but also by alterations in the PI3K/Akt pathway. Taken together, the downregulated expression of miR-145 in thyroid cancer is likely to contribute to the complex cascade of events associated with thyroid cancer angiogenesis via its effect on *VEGF* and *HIF1α* expression, and Akt phosphorylation.

The reduction in stem cell markers we observed with miR-145 overexpression was accompanied with decreased expression of thyroid cell differentiation markers. This observation suggests that miR-145 decreases stem-like properties and may reverse the differentiation of thyroid cancer cells. These data are consistent with recent studies that have demonstrated that miR-145 inhibits cancer stem cell characteristics (Huang *et al*. 2012).

Our functional study results with miR-145 overexpression and inhibition can be explained by the effect of miR-145 on the PI3K/Akt pathway. Accumulating evidence indicates that the PI3K/Akt pathway regulates EMT, cell cycle, angiogenesis, and apoptosis (Chandramohan *et al*. 2004, Onoue *et al*. 2006, Fang *et al*. 2007, Cheng *et al*. 2008). Phosphorylated Akt activates mTOR, a major regulator of protein translation. Akt stabilizes cyclin D1, which antagonizes cyclin-dependent kinase inhibitors p21 and p27. Akt further prevents apoptosis by increasing the level of anti-apoptotic proteins BCL2 and BCL-xL, while inactivating proapoptotic proteins such as BAD, BAX, and BIM (Datta *et al*. 1997, Maddika *et al*. 2007). The current study shows that miR-145 expression leads to the inhibition of Akt phosphorylation, accumulation of p21, and inhibition of *HIF1α* and *VEGF* expression. Thus, we propose that, because mutations in the PI3K/Akt are relatively rare in thyroid cancer, a primary event such as the loss of miR-145 expression could mediate the multiple effects of increased activation of p-Akt Ser^{473}. Our data indicate that PI3K/Akt is directly targeted by miR-145 through the post-transcriptional regulation of Akt3.

We also present evidence showing that the activation of p-Akt downregulates miR-145 expression. This finding indicates that miR-145 is involved in the negative feedback regulation of the PI3k/Akt pathway. Moreover, a few studies describe the regulatory interactions between miRNAs and their targets, suggesting that miRNAs can autoregulate their expression through negative feedback regulation (Johnston *et al*. 2005, Li *et al*. 2011). Our data are consistent with previous studies showing that PI3K/Akt inhibitor or resveratrol treatment inhibits p-Akt and induces miR-145. Although several transcription factors, such as Foxo and p53, have been implicated in the regulation of miR-145, the silencing of miR-145 in many cancers is not clearly understood (Gan *et al*. 2010, Ren *et al*. 2013). The specific inhibition of the PI3K/Akt pathway has been recently reported to lead to upregulation of miR-145 in a p53-dependent manner (Sachdeva *et al*. 2009). However, two of the cell lines used in our study (8505C and FTC-133) have p53 mutation (C→G and G→A respectively), and both are located in the DNA-binding domain of the protein (Wright *et al*. 1991, Yoshimoto *et al*. 1992). Thus, in contrast to the previous findings, we believe the role of PI3K/Akt in miR-145 expression is not likely to be dependent on p53 in thyroid cancer cells.

Because of the role (of miR-145 in thyroid cancer biology) we observed, we hypothesized that miR-145 could serve as a candidate biomarker in the diagnosis of thyroid cancer. Thyroid nodule FNA biopsy is considered the most accurate tool for differentiating between benign and malignant thyroid nodules. However, it is inconclusive in ~30% of biopsies. Our data indicated that miR-145 expression is significantly lower in malignant thyroid nodules, with a sensitivity of 96% and low specificity of 27%, but with a high NPV of 92%. While the low specificity would lead to a large number of false positive tests, screening for miR-145 expression could be an effective test in patients with inconclusive FNA biopsies; if the expression level is high, a thyroid cancer diagnosis could be excluded. Further studies are warranted to validate the clinical utility of measuring miR-145 in thyroid FNA biopsy samples.

Beyond the utility of measuring miRNAs as markers in thyroid FNA biopsy, studies have reported the potential of measuring circulating miRNA as biomarkers (Brase *et al*. 2010). Our data indicate that the level of miR-145 is higher in the serum of patients with PTC. In contrast, miR-145 was downregulated in tissues samples. Our finding is consistent with high levels of miR-145 in serum of patients with colorectal cancer compared to controls; however, others studies have reported downregulation of miR-145 in colorectal cancer tissue compared with nontumor tissues (Bandres *et al*. 2006, Wang *et al*. 2012, Luo *et al*. 2013). These findings suggest that miR-145 is either actively secreted by the tumor cell or released passively through the cell membranes. Indeed, several investigators have suggested that circulating miRNAs are stabilized by AGO2 protein, protected from RNAse degradation by encapsulation in exosomes

http://erc.endocrinology-journals.org
DOI: 10.1530/ERC-14-0077

Published by Bioscientifica Ltd.

(Valadi *et al*. 2007). The findings from our *in vitro* studies using chemical Golgi inhibitor and ceramide biosynthesis inhibitor and *in vivo* venous gradient samples in patients with PTC suggest that miR-145 is secreted in exosomes by thyroid cancer cells. Thus, we believe that the high serum levels observed in patients with PTC are due to the active secretion of miR-145.

In conclusion, our data demonstrate that miR-145 has a tumor-suppressor function and directly targets AKT3 to regulate the PI3K/Akt signaling pathway. miR-145 regulates multiple hallmarks of malignancy *in vitro* and *in vivo*, suppressing the growth and metastasis of thyroid cancer cells. Furthermore, lower expression of miR-145 in FNA biopsy samples has a high NPV, which could be clinically useful for excluding a thyroid cancer diagnosis. The high levels of miR-145 in serum samples of patients with PTC provides new insights into the mechanisms of loss of expression of tumor-suppressor miRNAs that occur in the tumor itself as a result of cellular excretion. Thus, miR-145 is promising both in furthering our understanding of thyroid cancer biology and as a useful diagnostic marker and target for thyroid cancer therapy.

Supplementary data

This is linked to the online version of the paper at http://dx.doi.org/10.1530/ERC-14-0077.

Declaration of interest

The authors declare that there is no conflict of interest that could be perceived as prejudicing the impartiality of the research reported.

Funding

This research was supported by the intramural research program of the Center for Cancer Research, National Cancer Institute, National Institutes of Health.

Author contribution statement

M Boufraqech and E Kebebew developed the hypothesis, designed the experiments, wrote and edited the manuscript. M Boufraqech, L Zhang, and M Jain performed the experiments. D Patel and R Ellis contributed to the manuscript editing. E Kebebew, N Nilubol, and D Patel provided patient samples. N Nilubol contributed to the data analysis. M He and Y Xiong contributed to the acquisition of the data. M J Merino contributed to the pathology review and interpretation.

References

Akao Y, Nakagawa Y & Naoe T 2006 MicroRNAs 143 and 145 are possible common onco-microRNAs in human cancers. *Oncology Reports* **16** 845–850. (doi:10.3892/or.16.4.845)

Bandres E, Cubedo E, Agirre X, Malumbres R, Zarate R, Ramirez N, Abajo A, Navarro A, Moreno I, Monzo M *et al*. 2006 Identification by real-time PCR of 13 mature microRNAs differentially expressed in colorectal cancer and non-tumoral tissues. *Molecular Cancer* **5** 29. (doi:10.1186/1476-4598-5-29)

Brase JC, Wuttig D, Kuner R & Sultmann H 2010 Serum microRNAs as non-invasive biomarkers for cancer. *Molecular Cancer* **9** 306. (doi:10.1186/1476-4598-9-306)

Burrows N, Resch J, Cowen RL, von Wasielewski R, Hoang-Vu C, West CM, Williams KJ & Brabant G 2010 Expression of hypoxia-inducible factor 1α in thyroid carcinomas. *Endocrine-Related Cancer* **17** 61–72. (doi:10.1677/ERC-08-0251)

Ceppi P & Peter ME 2014 MicroRNAs regulate both epithelial-to-mesenchymal transition and cancer stem cells. *Oncogene* **33** 269–278. (doi:10.1038/onc.2013.55)

Chandramohan V, Jeay S, Pianetti S & Sonenshein GE 2004 Reciprocal control of Forkhead box O 3a and c-Myc via the phosphatidylinositol 3-kinase pathway coordinately regulates p27Kip1 levels. *Journal of Immunology* **172** 5522–5527. (doi:10.4049/jimmunol.172.9.5522)

de la Chapelle A & Jazdzewski K 2011 MicroRNAs in thyroid cancer. *Journal of Clinical Endocrinology and Metabolism* **96** 3326–3336. (doi:10.1210/jc.2011-1004)

Cheng GZ, Park S, Shu S, He L, Kong W, Zhang W, Yuan Z, Wang LH & Cheng JQ 2008 Advances of AKT pathway in human oncogenesis and as a target for anti-cancer drug discovery. *Current Cancer Drug Targets* **8** 2–6. (doi:10.2174/156800908783497104)

Cibas ES & Ali SZ 2009 The Bethesda system for reporting thyroid cytopathology. *Thyroid* **19** 1159–1165. (doi:10.1089/thy.2009.0274)

Datta SR, Dudek H, Tao X, Masters S, Fu H, Gotoh Y & Greenberg ME 1997 Akt phosphorylation of BAD couples survival signals to the cell-intrinsic death machinery. *Cell* **91** 231–241. (doi:10.1016/S0092-8674(00)80405-5)

De Craene B & Berx G 2013 Regulatory networks defining EMT during cancer initiation and progression. *Nature Reviews. Cancer* **13** 97–110. (doi:10.1038/nrc3447)

Fan L, Wu Q, Xing X, Wei Y & Shao Z 2012 MicroRNA-145 targets vascular endothelial growth factor and inhibits invasion and metastasis of osteosarcoma cells. *Acta Biochimica et Biophysica Sinica* **44** 407–414. (doi:10.1093/abbs/gms019)

Fang J, Ding M, Yang L, Liu LZ & Jiang BH 2007 PI3K/PTEN/AKT signaling regulates prostate tumor angiogenesis. *Cellular Signalling* **19** 2487–2497. (doi:10.1016/j.cellsig.2007.07.025)

Gan B, Lim C, Chu G, Hua S, Ding Z, Collins M, Hu J, Jiang S, Fletcher-Sananikone E, Zhuang L *et al*. 2010 FoxOs enforce a progression checkpoint to constrain mTORC1-activated renal tumorigenesis. *Cancer Cell* **18** 472–484. (doi:10.1016/j.ccr.2010.10.019)

Huang S, Guo W, Tang Y, Ren D, Zou X & Peng X 2012 miR-143 and miR-145 inhibit stem cell characteristics of PC-3 prostate cancer cells. *Oncology Reports* **28** 1831–1837. (doi:10.3892/or.2012.2015)

Islam A, Shen X, Hiroi T, Moss J, Vaughan M & Levine SJ 2007 The brefeldin A-inhibited guanine nucleotide-exchange protein, BIG2, regulates the constitutive release of TNFR1 exosome-like vesicles. *Journal of Biological Chemistry* **282** 9591–9599. (doi:10.1074/jbc.M607122200)

Johnston RJ Jr, Chang S, Etchberger JF, Ortiz CO & Hobert O 2005 MicroRNAs acting in a double-negative feedback loop to control a neuronal cell fate decision. *PNAS* **102** 12449–12454. (doi:10.1073/pnas.0505530102)

Kitano M, Rahbari R, Patterson EE, Steinberg SM, Prasad NB, Wang Y, Zeiger MA & Kebebew E 2012 Evaluation of candidate diagnostic microRNAs in thyroid fine-needle aspiration biopsy samples. *Thyroid* **22** 285–291. (doi:10.1089/thy.2011.0313)

Lacroix L, Michiels S, Mian C, Arturi F, Caillou B, Filetti S, Schlumberger M & Bidart JM 2006 HEX, PAX-8 and TTF-1 gene expression in human thyroid tissues: a comparative analysis with other genes involved in iodide metabolism. *Clinical Endocrinology* **64** 398–404. (doi:10.1111/j.1365-2265.2006.02477.x)

Published by Bioscientifica Ltd.

Li Y, Zhang H & Chen Y 2011 MicroRNA-mediated positive feedback loop and optimized bistable switch in a cancer network involving miR-17-92. *PLoS ONE* **6** e26302. (doi:10.1371/journal.pone.0026302)

Luo X, Stock C, Burwinkel B & Brenner H 2013 Identification and evaluation of plasma microRNAs for early detection of colorectal cancer. *PLoS ONE* **8** e62880. (doi:10.1371/journal.pone.0062880)

Maddika S, Ande SR, Panigrahi S, Paranjothy T, Weglarczyk K, Zuse A, Eshraghi M, Manda KD, Wiechec E & Los M 2007 Cell survival, cell death and cell cycle pathways are interconnected: implications for cancer therapy. *Drug Resistance Updates* **10** 13–29. (doi:10.1016/j.drup.2007.01.003)

Mitchell PS, Parkin RK, Kroh EM, Fritz BR, Wyman SK, Pogosova-Agadjanyan EL, Peterson A, Noteboom J, O'Briant KC, Allen A *et al.* 2008 Circulating microRNAs as stable blood-based markers for cancer detection. *PNAS* **105** 10513–10518. (doi:10.1073/pnas.0804549105)

Ng EK, Chong WW, Jin H, Lam EK, Shin VY, Yu J, Poon TC, Ng SS & Sung JJ 2009 Differential expression of microRNAs in plasma of patients with colorectal cancer: a potential marker for colorectal cancer screening. *Gut* **58** 1375–1381. (doi:10.1136/gut.2008.167817)

Onoue T, Uchida D, Begum NM, Tomizuka Y, Yoshida H & Sato M 2006 Epithelial–mesenchymal transition induced by the stromal cell-derived factor-1/CXCR4 system in oral squamous cell carcinoma cells. *International Journal of Oncology* **29** 1133–1138. (doi:10.3892/ijo.29.5.1133)

Pallante P, Visone R, Ferracin M, Ferraro A, Berlingieri MT, Troncone G, Chiappetta G, Liu CG, Santoro M, Negrini M *et al.* 2006 MicroRNA deregulation in human thyroid papillary carcinomas. *Endocrine-Related Cancer* **13** 497–508. (doi:10.1677/erc.1.01209)

Pallante P, Battista S, Pierantoni GM & Fusco A 2014 Deregulation of microRNA expression in thyroid neoplasias. *Nature Reviews. Endocrinology* **10** 88–101. (doi:10.1038/nrendo.2013.223)

Patel KN & Shaha AR 2006 Poorly differentiated and anaplastic thyroid cancer. *Cancer Control* **13** 119–128.

Ren D, Wang M, Guo W, Zhao X, Tu X, Huang S, Zou X & Peng X 2013 Wild-type p53 suppresses the epithelial–mesenchymal transition and stemness in PC-3 prostate cancer cells by modulating miR145. *International Journal of Oncology* **42** 1473–1481. (doi:10.3892/ijo.2013.1825)

Sachdeva M, Zhu S, Wu F, Wu H, Walia V, Kumar S, Elble R, Watabe K & Mo YY 2009 p53 represses c-Myc through induction of the tumor suppressor miR-145. *PNAS* **106** 3207–3212. (doi:10.1073/pnas.0808042106)

Schlumberger M 2007 Papillary and follicular thyroid carcinoma. *Annales d'Endocrinologie* **68** 120–128. (doi:10.1016/j.ando.2007.04.004)

Soh EY, Duh QY, Sobhi SA, Young DM, Epstein HD, Wong MG, Garcia YK, Min YD, Grossman RF, Siperstein AE *et al.* 1997 Vascular endothelial growth factor expression is higher in differentiated thyroid cancer than in normal or benign thyroid. *Journal of Clinical Endocrinology and Metabolism* **82** 3741–3747. (doi:10.1210/jcem.82.11.4340)

Solomides CC, Evans BJ, Navenot JM, Vadigepalli R, Peiper SC & Wang ZX 2012 MicroRNA profiling in lung cancer reveals new molecular markers for diagnosis. *Acta Cytologica* **56** 645–654. (doi:10.1159/000343473)

Spaderna S, Schmalhofer O, Hlubek F, Berx G, Eger A, Merkel S, Jung A, Kirchner T & Brabletz T 2006 A transient, EMT-linked loss of basement membranes indicates metastasis and poor survival in colorectal cancer. *Gastroenterology* **131** 830–840. (doi:10.1053/j.gastro.2006.06.016)

Theoharis C, Roman S & Sosa JA 2012 The molecular diagnosis and management of thyroid neoplasms. *Current Opinion in Oncology* **24** 35–41. (doi:10.1097/CCO.0b013e32834dcfca)

Trajkovic K, Hsu C, Chiantia S, Rajendran L, Wenzel D, Wieland F, Schwille P, Brugger B & Simons M 2008 Ceramide triggers budding of exosome vesicles into multivesicular endosomes. *Science* **319** 1244–1247. (doi:10.1126/science.1153124)

Tuttle RM, Fleisher M, Francis GL & Robbins RJ 2002 Serum vascular endothelial growth factor levels are elevated in metastatic differentiated thyroid cancer but not increased by short-term TSH stimulation. *Journal of Clinical Endocrinology and Metabolism* **87** 1737–1742. (doi:10.1210/jcem.87.4.8388)

Valadi H, Ekstrom K, Bossios A, Sjostrand M, Lee JJ & Lotvall JO 2007 Exosome-mediated transfer of mRNAs and microRNAs is a novel mechanism of genetic exchange between cells. *Nature Cell Biology* **9** 654–659. (doi:10.1038/ncb1596)

Viglietto G, Maglione D, Rambaldi M, Cerutti J, Romano A, Trapasso F, Fedele M, Ippolito P, Chiappetta G, Botti G *et al.* 1995 Upregulation of vascular endothelial growth factor (VEGF) and downregulation of placenta growth factor (PlGF) associated with malignancy in human thyroid tumors and cell lines. *Oncogene* **11** 1569–1579.

Volinia S, Calin GA, Liu CG, Ambs S, Cimmino A, Petrocca F, Visone R, Iorio M, Roldo C, Ferracin M *et al.* 2006 A microRNA expression signature of human solid tumors defines cancer gene targets. *PNAS* **103** 2257–2261. (doi:10.1073/pnas.0510565103)

Wang Z, Zhang X, Yang Z, Du H, Wu Z, Gong J, Yan J & Zheng Q 2012 MiR-145 regulates PAK4 via the MAPK pathway and exhibits an anti-tumor effect in human colon cells. *Biochemical and Biophysical Research Communications* **427** 444–449. (doi:10.1016/j.bbrc.2012.06.123)

Wright PA, Lemoine NR, Goretzki PE, Wyllie FS, Bond J, Hughes C, Roher HD, Williams ED & Wynford-Thomas D 1991 Mutation of the p53 gene in a differentiated human thyroid carcinoma cell line, but not in primary thyroid tumours. *Oncogene* **6** 1693–1697.

Xu Q, Liu LZ, Qian X, Chen Q, Jiang Y, Li D, Lai L & Jiang BH 2012 MiR-145 directly targets p70S6K1 in cancer cells to inhibit tumor growth and angiogenesis. *Nucleic Acids Research* **40** 761–774. (doi:10.1093/nar/gkr730)

Yang J, Dai C & Liu Y 2005 A novel mechanism by which hepatocyte growth factor blocks tubular epithelial to mesenchymal transition. *Journal of the American Society of Nephrology* **16** 68–78. (doi:10.1681/ASN.2003090795)

Yoshimoto K, Iwahana H, Fukuda A, Sano T, Saito S & Itakura M 1992 Role of p53 mutations in endocrine tumorigenesis: mutation detection by polymerase chain reaction-single strand conformation polymorphism. *Cancer Research* **52** 5061–5064.

Zhang J, Sun Q, Zhang Z, Ge S, Han ZG & Chen WT 2013 Loss of microRNA-143/145 disturbs cellular growth and apoptosis of human epithelial cancers by impairing the MDM2-p53 feedback loop. *Oncogene* **32** 61–69. (doi:10.1038/onc.2012.28)

Zhong WB, Liang YC, Wang CY, Chang TC & Lee WS 2005 Lovastatin suppresses invasiveness of anaplastic thyroid cancer cells by inhibiting Rho geranylgeranylation and RhoA/ROCK signaling. *Endocrine-Related Cancer* **12** 615–629. (doi:10.1677/erc.1.01012)

Received in final form 15 April 2014
Accepted 23 April 2014
Made available online as an Accepted Preprint
29 April 2014

Published by Bioscientifica Ltd.